Resolution Limits in Broadband Incoherent Correlation Imaging

Petr Bouchal^{1,*}, Zdeněk Bouchal², Radim Chmelík¹ ¹Central European Institute of Technology, Brno University of Technology, Technická 10, 616 00 Brno, Czech Republic ²Department of Optics, Palacký University, 17. listopadu 1192/12, 771 46 Olomouc, Czech Republic *E-mail: petr.bouchal@ceitec.vutbr.cz

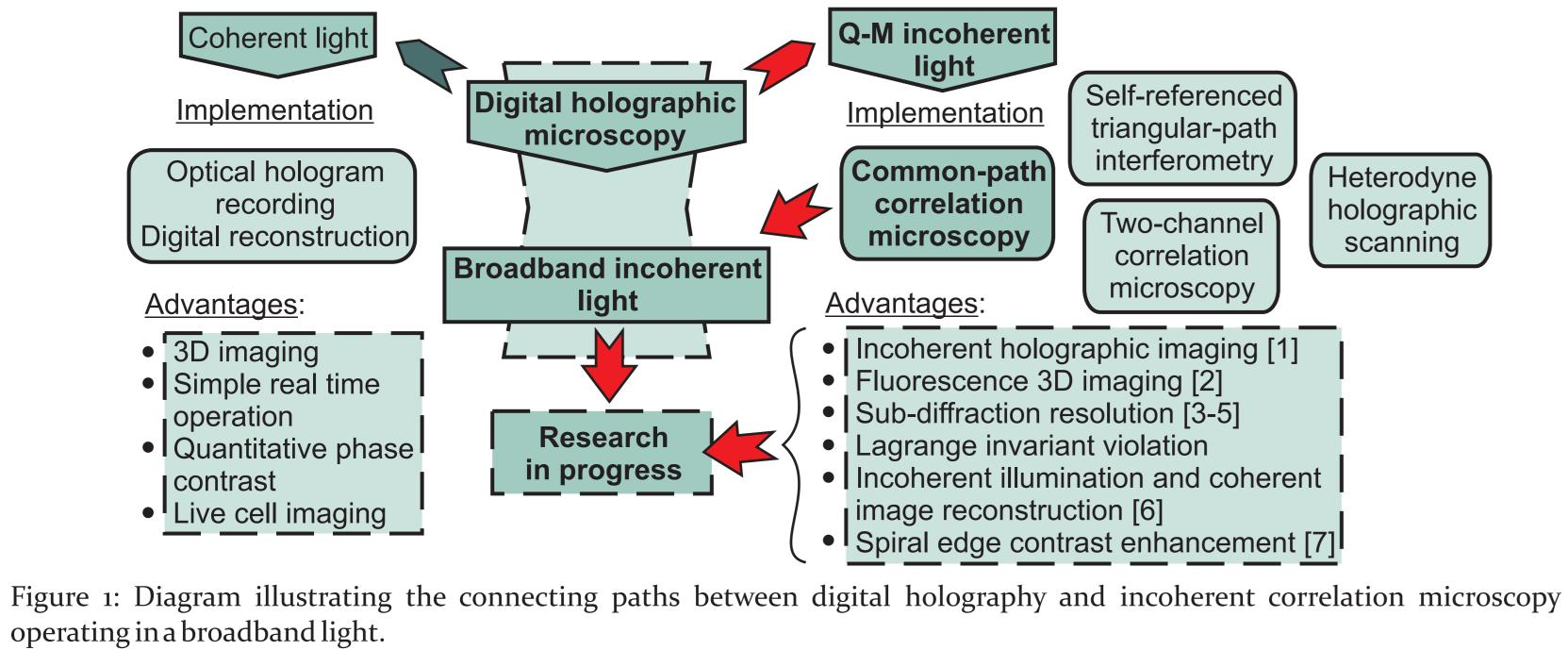
echnology Agency

RNO CZECH REPUBLIC



Novel avenues in the digital correlation imaging

Recent progress in digital holography has been supported by proposals for new experiments, advanced technologies for light shaping and development of methods for data acquisition and processing. This effort has given rise to new techniques allowing to use the 3D holographic reconstruction principles also in the Q-M spatially incoherent light. Here, further progress is outlined, leading to the sub-diffraction resolution in white light correlation imaging. A brief overview of methods demonstrating recent development and applications of the coherent and incoherent digital holographic microscopy is shown in Fig. 1.



operating in a broadband light.

The Q-M common-path correlation microscopy

In the Q-M correlation imaging, the holographic records of separate object points are acquired in the common-path interferometer enabling a wavefront splitting. If the OPD of the created signal and reference waves does not exceed the CL, the waves interfere and the Fresnel holograms of all points of the 3D object are created simultaneously without scanning. After processing of three phase-shifted recordings of the object, the digital image reconstruction is performed.

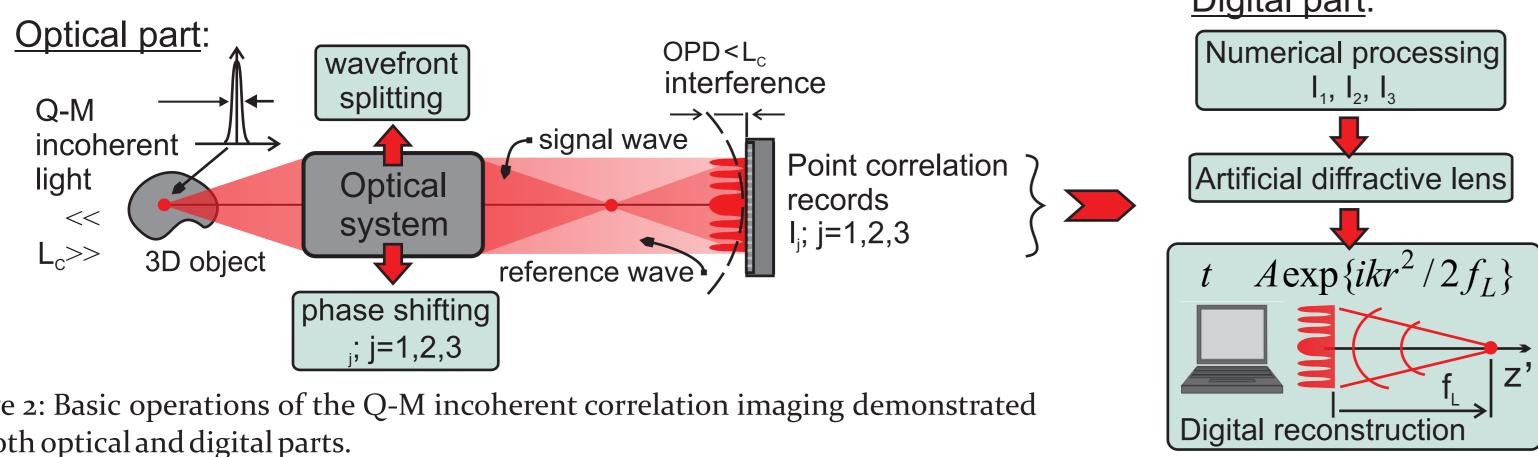


Figure 2: Basic operations of the Q-M incoherent correlation imaging demonstrated for both optical and digital parts.

Experimental configurations of the common-path correlation microscopy

Recently, the Fresnel Incoherent Correlation Holography (FINCH) was proposed for experimental realization of the holographic imaging of incoherently illuminated 3D objects [1]. In this set-up, the wavefront splitting is carried out by a SLM, which allows operating changes in the geometry of the interfering waves in order to achieve an optimal configuration with the significantly reduced OPD.

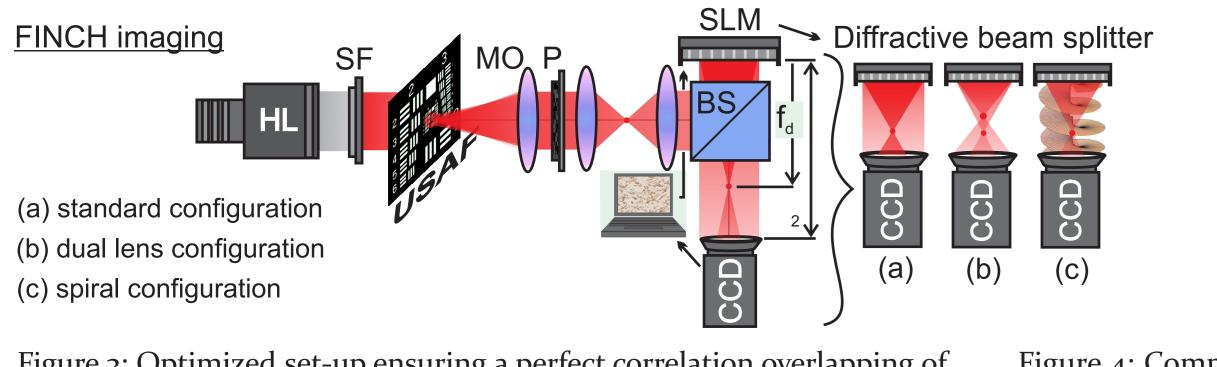
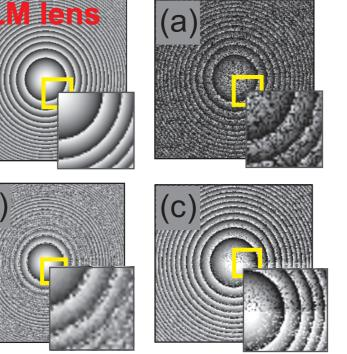


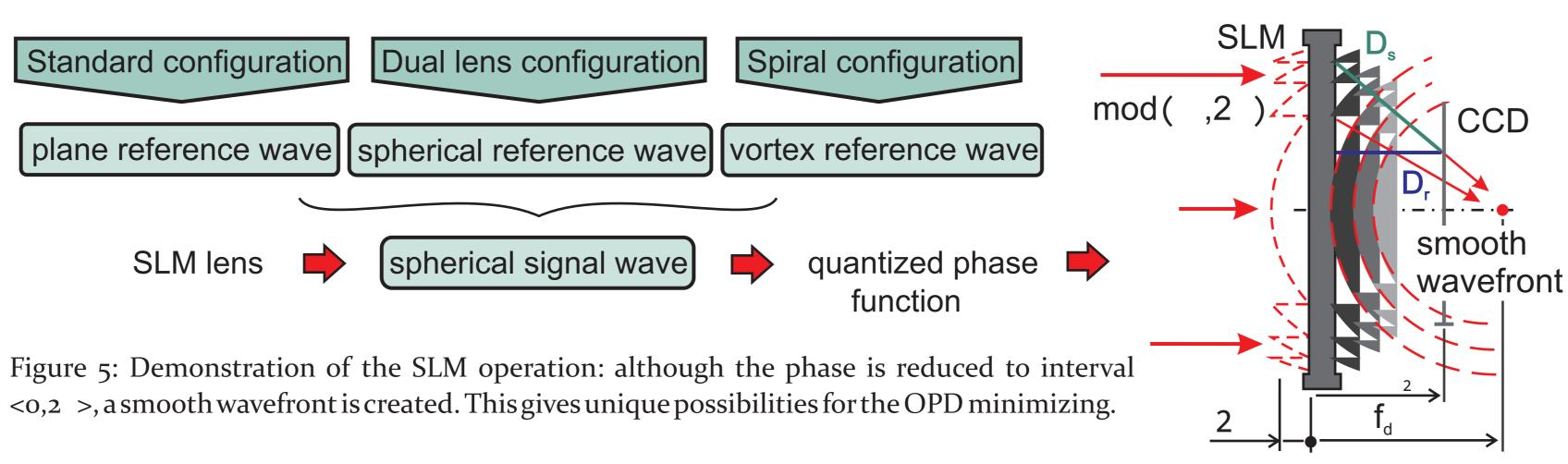


Figure 4: Computer generated holograms used in the basic imaging modes.

[1] J. Rosen and G. Brooker, Digital spatially incoherent Fresnel holography, Opt. Lett. 32, 912-914 (2007). [7] P. Bouchal and Z. Bouchal, Selective edge enhancement in three-dimensional vortex imaging with incoherent light, Opt. Lett. 37, 2949-2951 (2012). [2] J. Rosen and G. Brooker, Fluorescence incoherent color holography, Opt. Express 15, 2244-2250 (2007). [8] P. Bouchal and Z. Bouchal, Wide-field common-path incoherent correlation microscopy with a perfect overlapping of interfering beams, J. Europ. Opt. Soc. Rap. Public. 8, 1300 (2013). [3] J. Rosen, N. Siegel, and G. Brooker, Theoretical and experimental demonstration of resolution beyond the Rayleigh limit by FINCH fluorescence microscopic imaging, Opt. Express 19, 26249-26268 (2011). [4] B. Katz, J. Rosen, R. Kelner, and G. Brooker, Enhanced resolution and throughput of Fresnel incoherent correlation holography (FINCH) using dual diffractive lenses on a spatial light modulator (SLM), Opt. Express 20, 9109-9121 (2012) This work was supported by the Technology Agency of the Czech Republic, project No .TE 0 1 0 2 0 2a add the project CEITEC - "Central European Institute of Technology" No .CZ . 1 . 0 5 / 1 . 1 . 0 footh @ a operation Regional [5] X. Lai, Y. Zhao, X. Lv, Z. Zhou, and S. Zeng, Fluorescence holography with improved signal-to-noise ratio by near image plane recording, Opt. Lett. 37, 2445–2447 (2012). Development Fund. [6] P. Bouchal, J. Kapitán, R. Chmelík, and Z. Bouchal, Point spread function and two-point resolution in Fresnel incoherent correlation holography, Opt. Express 19, 15603-15620 (2011).

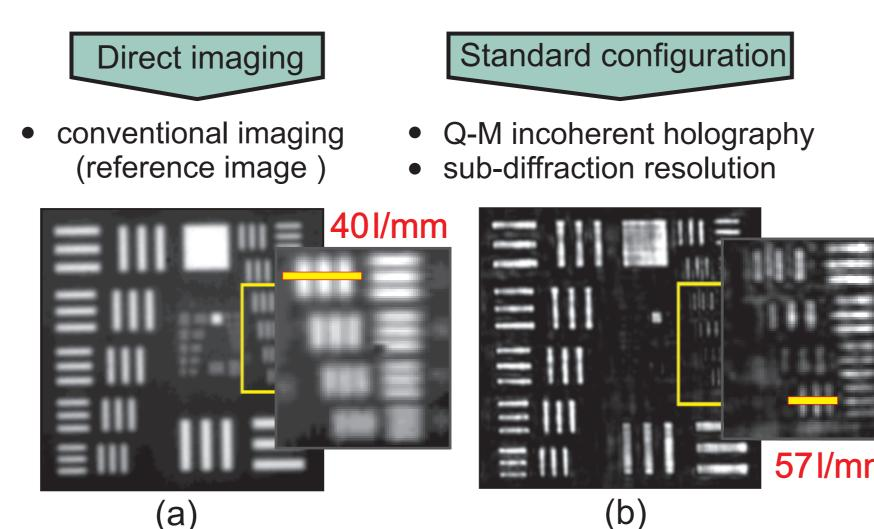
Digital part:





Experimental results

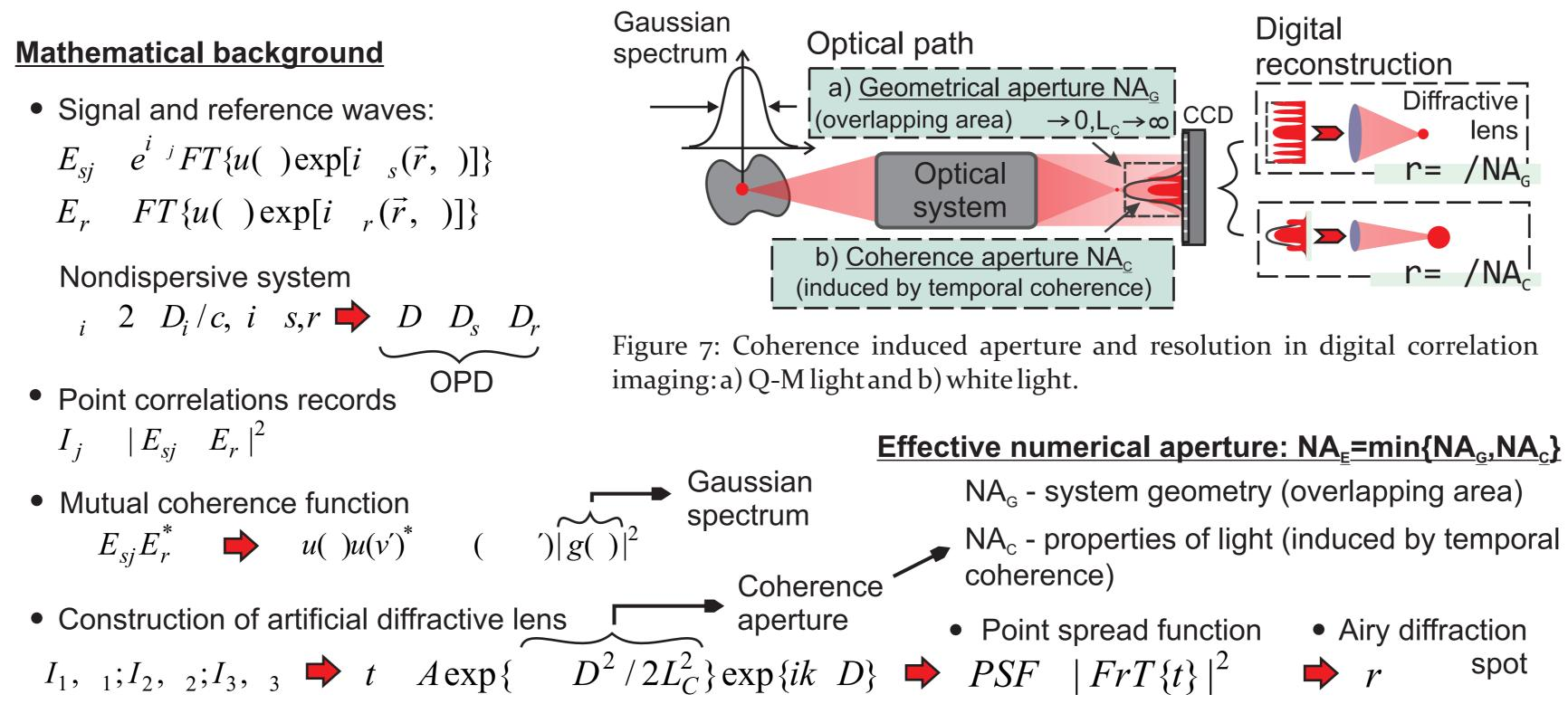
FINCH is a powerful method that brings new benefits to the incoherent holographic microscopy and is especially promising for fluorescence microscopy. Due to a variability of the method, various imaging modes can be switched almost in real time.



standard image, c) dual lens image, d) spiral image with edge contrast ennhancement [7].

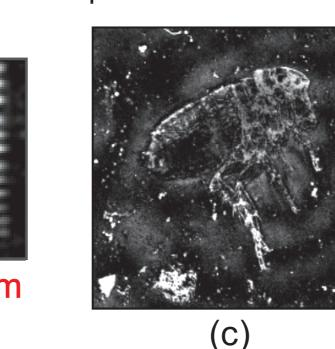
Resolution limits in broadband correlation imaging

In correlation imaging, three phase shifted interference patterns are recorded for each point of the object. After numerical processing, an artificial diffractive lens is created whose numerical aperture determines the resolution of the digitally reconstructed image. In the Q-M light, the resolution is limited by the geometrical aperture (GA) given by an overlapping area of interfering waves. In the broadband light, the coherence aperture (CA) depending on both the CL and the OPD determines the image resolution (Fig. 7).



Dual lens configuration

 sub-diffraction resolution • spectral resistance



Spiral configuration

edge enhancement in

3D incoherent imaging

Figure 6: Images reconstructed from experimental records obtained in various FINCH configurations: a) reference optical image, b)

Abstract: In recent years, the digital holography has been supplemented by new techniques enabling operation in a quasi-monochromatic (Q-M) spatially incoherent light. Here, the basic imaging modes and advantages of the common-path correlation microscopy using a spatial light modulator (SLM) are presented for both the Q-M and broadband light. Based on the proposed concept of the coherence aperture (CA), the interconnection between experiment geometry, optical path difference (OPD), source coherence length (CL) and the image resolution is established. As the main result, the experimental conditions of the white light correlation microscopy are found under which the sub-diffraction resolution can be achieved.

Resolution in the standard FINCH

The best resolution obtained with Q-M and broadband light requires different CCD positioning given by 2.

The optimal CCD setting for the Q-M light

At the CCD position optimal for the Q-M light (point (a) in Fig. 9), the resolution is strongly reduced when the broadband light is used (NA_F=NA_C, point (b) in Fig. 9)

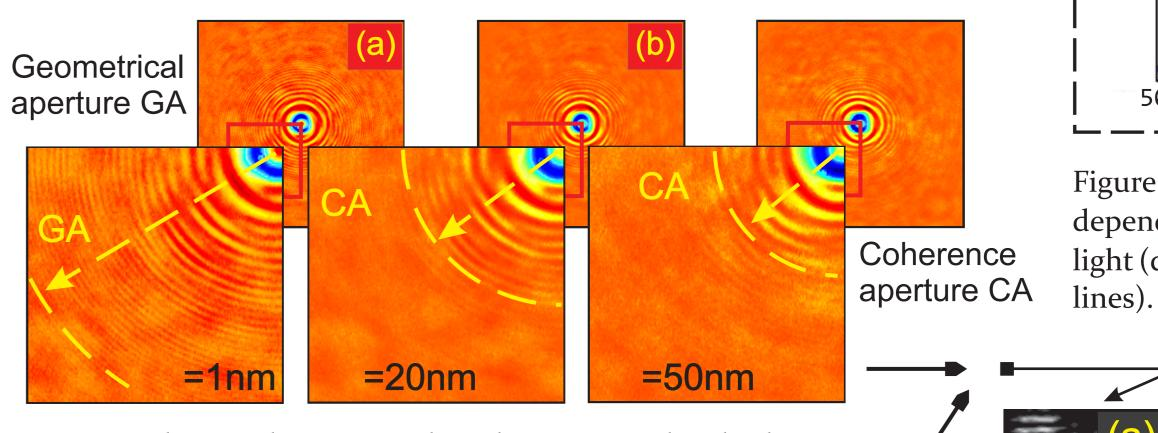


Figure 8: The correlation records with geometrical and coherence apertures: (a) and (b) taken at equally denoted points in Fig. 9.

The optimal CCD setting for the broadband light

In distant CCD positions, the resolution for the Q-M light is maintained even when the broadband light is used ($NA_{F}=NA_{G}$, points (c) and (d) in Fig. 9).

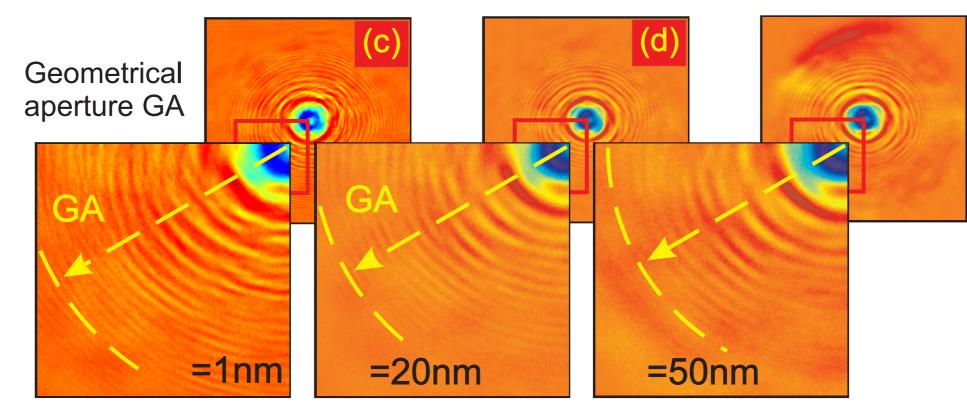
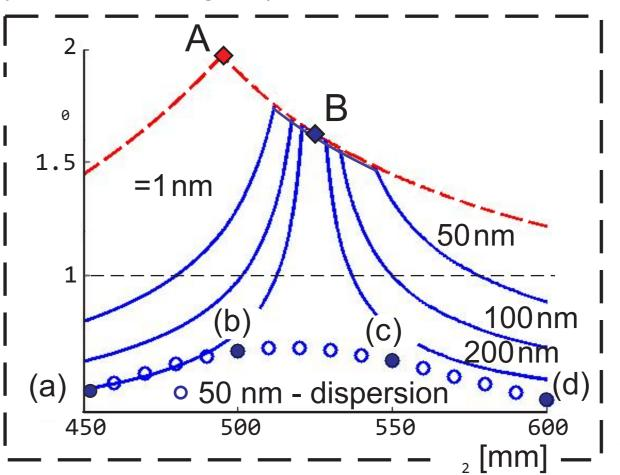


Figure 10: The correlation records captured at positions where the temporal coherence does not reduce the resolution: (c) and (d) taken at equally denoted points in Fig. 9.

Resolution in the dual lens FINCH

In this configuration, the resolution twice overcoming the diffraction limit was demonstrated with the Q-M light in optimal CCD position [4,5] (point A in Fig. 12). When using the broadband light, the resolution is strongly reduced in improper CCD positions (solid lines in Fig. 12), but remains the same as for the Q-M light in optimal CCD settings (near position B in Fig. 13).



Conclusions: The resolution of the broadband correlation imaging was analyzed with the following results: • connection between the temporal coherence and the resolution was established using concept of the coherence induced aperture, • CCD positions ensuring the best resolution in broadband light were found, • possibility of achieving sub-diffraction resolution in white light was discovered, provided that the aberrations and dispersion of the system are eliminated.

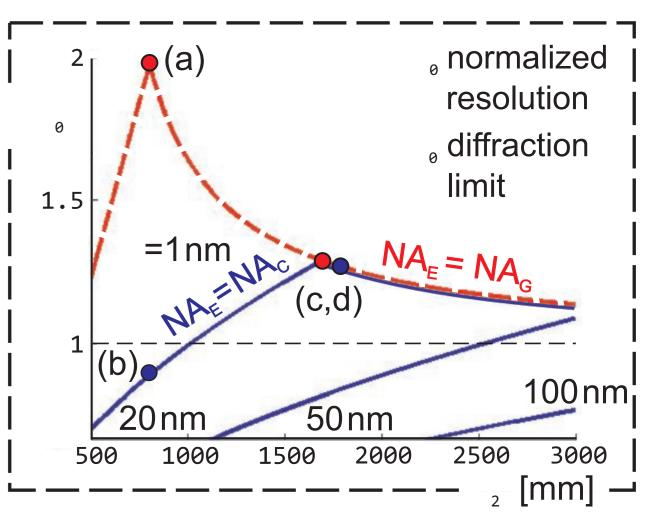


Figure 9: The normalized image resolution in dependence on the CCD position _____ for the Q-M light (dashed line) and the broadband light (solid

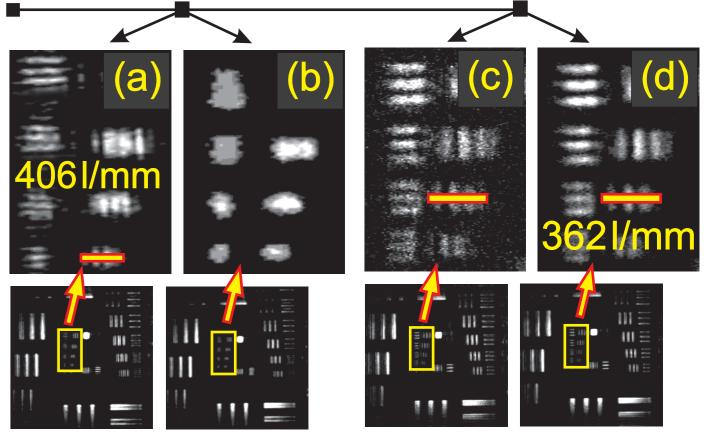


Figure 11: Reconstruction of the USAF target in the positions (a)-(d) in Fig. 9. Resolution obtained for =1nm and 20 nm is significantly different in the positions (a) and (b) but remains unchanged in the positions (c) and (d).

(a)

Figure 13: Experimental reconstruction of the USAF target affected by the SLM dispersion. The correlation records were taken in the positions (a) - (d) of Fig. 12.

For this setting, the sub-diffraction resolution is achieved even with the white light. This fascinating property is possible only when aberrations and dispersion of the system are eliminated. Theoretical evaluation of the resolution sensitivity to the SLM dispersion is shown in Fig. 12 (curve ooo). The experimental image reconstructions in points (a)-(d) are demonstrated in Fig. 13.

Figure 12: Image resolution in the Q-M light (dashed line), the broadband light without disperion (solid lines) and the broadband light with the SLM dispersion